Spatial maps of DCEMRI enhancement in endplates of degenerating intervertebral discs reveal major pathologic changes

Volkan Emre Arpinar[1], Ali Ersoz[2], and L Tugan Muftuler[1,3]

[1]*Department of Neurosurgery, Medical College of Wisconsin, Milwaukee, Wisconsin, United States,* [2]*Department of Boiphysics, Medical College of Wisconsin, Wisconsin, United States,* [3]*Center for Imaging Research, Medical College of Wisconsin, Wisconsin, United States*

Target Audience: This presentation is intended for clinicians and researchers who study spinal disc degeneration.

Introduction: Although it has been studied extensively, there is no consensus on the mechanisms of pathological intervertebral disc (IVD) degeneration or how it should be distinguished from the normal aging processes. One probable cause is poor nutrient transport to the disc through the endplates (EP), which is a cartilage layer positioned between the vertebral body (VB) and nucleus pulposus (NP)[1–3]. It is known that derangements in EP regions affect transport of gas and solutes into the disc[3] and it may initiate degeneration. In this study, Dynamic Contrast Enhanced MRI (DCEMRI) was used to investigate the relation between IVD degeneration and fluid/nutrient transport to the discs through the EPs and adjacent subchondral bones (SBs) of the VBs. We developed a standard space template for all lumbar EPs and SBs and registered each SB and EP onto this template in order to analyze spatial characteristics of degenerative changes across all subjects and lumbar levels. The ultimate goal is to understand aberrations in fluid/nutrient transport through the EPs and its contribution to the disc degeneration process.

Methods: 48 adult participants (Age(mean±std.dev.): 35±11y; 18 Females; Height:173±10cm; Weight:79±16kg) were scanned using a 3T GE MR750 (Waukesha, WI USA) system. The study was approved by the IRB and written consents were obtained from participants. DCEMRI data were acquired using a dual-echo FSPGR (16-sagittal slices with 3mm thickness, FOV=31cm, acquisition matrix=310×300, T_R=4.0ms, TE_1=1.1ms, TE_2=2.2ms, flip-angle=12°, 23 frames with 28s frame rate). The contrast (Gd-DTPA 0.1 mmol/kg) was administered manually as a bolus via an antecubital vein at the end of the 2nd dynamic frame. A T_2-weighted MRI was also acquired for grading of disc degeneration using Pfirrmann classification[4].Two radiologists and a trained medical student evaluated the discs and the median of grades was used for analysis. First, each DCEMRI image series were registered using 12-parameter affine transformation. Then, a trained operator manually drew regions of interest (ROI) on pre-contrast images of the DCEMRI to segment the 10 EPs and adjacent SBs in the lumbar area (Fig.1). Then, using these ROIs, planes parallel to the cranial and caudal faces of each lumbar IVD were determined and the integral of DCEMRI signal at each voxel was projected onto those planes for each EP and adjacent SB. A representative image slice with ROIs and projection planes (magenta line) are shown in Fig. 1. The projection images of all healthy subjects' discs (Grades I or II across all lumbar levels) were used to generate a standard template for each VB – disc interface surface. By taking the average of these surfaces, a template for disc surface was generated and named as standard-space disc surface. Each EP and SB was registered to this template for analysis. The discs were then grouped into 3 categories: healthy (Grade I or II), moderate degeneration (Grade III) and high degeneration (Grade IV or V) and average contrast enhancement maps for EPs and SBs were calculated for each group.

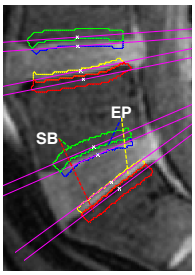

Fig.1. ROIs and IPs projection angles.

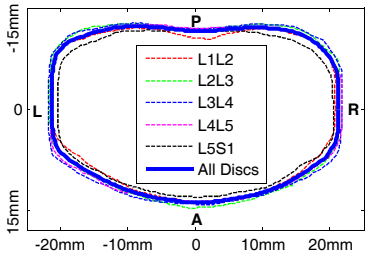

Fig.2. Different discs surface shapes and standard-space disc surface.

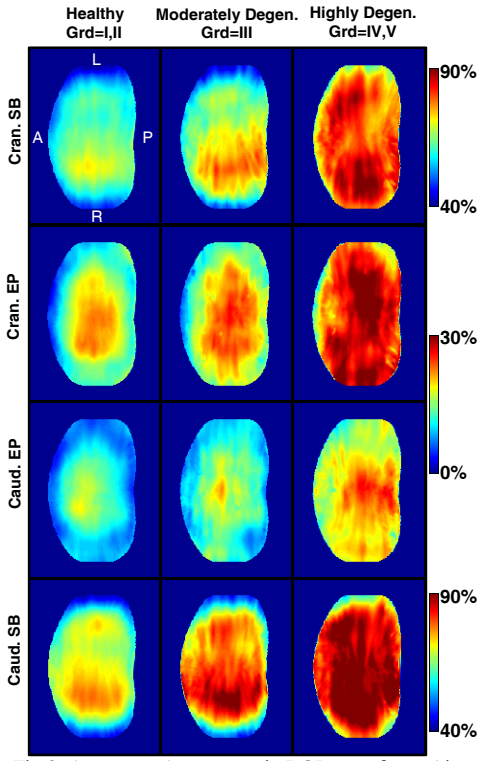

Fig.3. Average enhancement in ROIs transformed into standard-space disc surface with different degeneration.

Results: Template data was generated from 20 subjects (Age: 27±8y; 8 Females; Height: 171±10cm; Weight: 71±12kg) with healthy discs (Grade I or II) across all lumbar levels. The average surface shape for each lumbar disc is shown in Fig. 2 with dotted lines. As seen from the figure, the size differences between the discs were noticeable but their geometries were similar. Therefore, we used the average of all disc surfaces as the standard-space disc surface (shown with solid blue line). The average enhancement maps for each degeneration level are shown in Fig. 3. There were 169 healthy, 37 moderately degenerated and 34 highly degenerated discs. In this figure 0% represents no enhancement compared to the baseline image before contrast agent injection. Different color scales were used for EPs and adjacent SBs in this graph due to higher perfusion in SBs.

Discussion and Conclusion: Earlier ex vivo studies reported changes in porosity, pore diameter and trabecular thickness in the SB as the disc degenerates[5]. These changes lead to increased contrast agent uptake in SBs and EPs of degenerated discs. Our results also show that contrast agent uptake is higher in mid region compared to the periphery in the EPs. This is expected since the center region abuts the NP, where more diffusion is expected. Moreover, cranial EPs have higher enhancement compared to caudal EP in degenerating discs. This can be explained by a recent report that showed that the cranial EPs are more prone to fractures[6].

Use of the standard-space disc surface helped us analyze typical changes in VB – disc interface as discs degenerate. This method can be extended by using a pharmacokinetic model to understand actual pathophysiological changes in the endplate region. Ultimately, such techniques might help us understand the etiology of pathologic degeneration better and provide new information for more effective management of patients.

Acknowledgement: This study is supported by AOSpine SRN and Advancing a Healthier Wisconsin research grants.

References: **1.** Moon SM, et al. *Eur. Spine J.* 2013; 22:1820–28. **2.** Lotz JC, et al, *Glob. Spine J.* 2013; 3:153–64. **3.** Urban JP et al, *Spine* 2004; 29:2700-9. **4.** Pfirrmann CW, et al, *Spine* 2001; 26:1873–1878. **5.** Rodriguez AG, et al, *J. Orthop. Res.* 2012; 30:280–287. **6.** Zhao FD, et al, *Bone* 2009; 44(2):372-9.